



Stability of stainless steel sections under simple loading

Anne-Sophie Gagné¹, Lucile Gérard², Nicolas Boissonnade³

Abstract

The present paper investigates the resistance of stainless steel open sections as influenced by local stability issues. In particular, the influence of a rounded stress-strain law with large strain hardening effects on the buckling response of sections is studied. Several structural stainless steel grades are considered, as well as various section shapes under either compression or major-axis bending moment. The interaction between yielding and buckling is seen to be strongly influenced by individual element stability. Eventually, suitable design equations are proposed.

1 Introduction

The present paper relates to the behaviour, resistance and design of stainless steel open sections under simple loading, i.e. under either simple compression or under major-axis bending. Sections considered in the following are assumed fabricated by welding three stainless steel plates together, leading to doubly-symmetric sections.

More precisely, the main goal of this article consists in characterizing the key factors influencing the resistance of such sections to the most common and frequently-met types of loading. Of particular relevance is the influence of beneficial strain hardening effects, as well as the effects of premature local buckling; specific attention was therefore paid to quantify their impact on section resistance, eventually leading to the proposal of new, adequate design equations.

Although less frequently used than regular carbon steel, stainless steel has seen an increasing use in structural applications, mostly due to its durability, corrosion resistance, ease of maintenance aesthetics and fire resistance (Ashraf, 2006). In terms of resistance to compression and to bending, stainless steel open sections have recently received increased attention – in a non-exhaustive manner, one may cite the works of Ashraf (2006, 2006b), Afshan (2013), Gardner (2006, 2008), Young (2003, 2005), Real (2005) or Theofanous (2010). Among these works, the development of the Continuous Strength Method (C.S.M., Gardner, 2008) certainly stands as a corner stone within this topic, through its original strain-based approach that is particularly well suited to take the best advantage of the strain hardening reserves stemming from the rounded shape of the material stress-strain response. Consecutive to such research

¹ Undergraduate Student, Laval University, <anne-sophie.gagne.2@ulaval.ca>

² Graduate Student, Laval University, <lucile.gerard.1@ulaval.ca>

³ Professor, Laval University, <nicolas.boissonnade@gci.ulaval.ca>

investigations, major design codes now include sections specifically devoted to the design of stainless steel sections (AISC 2010, EN1993-1-4 2006, AS 4100 1998).

Besides, recent years have seen the development of a new, alternative design approach to steel sections and members: the Overall Interaction Concept (O.I.C., Boissonnade 2017, Hayeck 2018, Li 2017, Nseir 2015, Boissonnade 2014). Among other features, the O.I.C. (i) abandons the discrete and artificial cross-section classification concept, (ii) does not make use of the Effective Width Method, (iii) proposes a single, mechanically-based concept for the design of both sections and members, and (iv) allows all cross-section shapes (open or closed) to be treated similarly – the design procedures shall only differ in locally calibrated coefficients. Further, the concept clearly opens the door to computer-assisted design, since key R -ratios – see Fig. 1 and Fig. 8 – can nowadays be calculated by numerical tools.

The basic O.I.C. design principles are illustrated on Fig. 1. The actual loading on the section being known, one determines a relative slenderness λ_{rel} from a plastic load ratio R_{pl} (Step 1) and a critical load ratio R_{cr} (Step 2); this λ_{rel} value is then used to deduce a buckling factor χ (“penalty factor”) from a suitable “buckling curve” (Step 4). χ aims at accounting for a reduction on the plastic resistance owing to buckling effects – at the cross-section level in the present paper. The final design check (Step 5) consists in verifying that the reduced load ratio R_b still remains higher than unity, i.e. the loading acting on the section ought to be increased to exceed available resistance. In its principle, this approach is very similar to many recent design recommendations for member buckling.

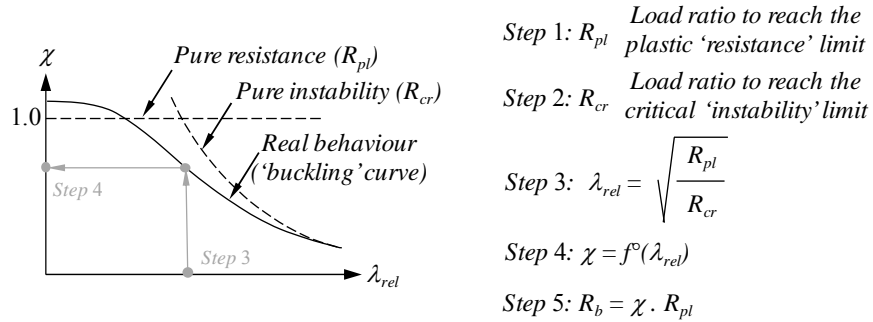


Figure 1: Basic principles and application steps of the O.I.C.

The O.I.C. can be seen as a major improvement brought to structural engineers and designers since, further to the above-listed advantages, it was shown to lead to a more economic design (Nseir 2015, Hayeck 2016). The present paper further extends the O.I.C. to the case of stainless steel sections, for which the material response is characterized by no plastic plateau and by significant strain hardening reserves. These particularities can be easily implemented in an O.I.C.-type approach in keeping a reference to plastic resistance through the conventional 0.2% material proof stress $\sigma_{0.2}$ while allowing for resistances higher than the plastic capacity through allowing for $\chi_L > 1.0$ values.

In this respect, numerical investigations were undertaken so as to provide O.I.C.-based design equations to predict the resistance of open stainless steel sections under simple loading. Next section 2 details the shell F.E. models used to provide reference results as well as the parameters considered in the study. Section 3 is devoted to recall the essentials and key features of established design approaches that will also be kept in the following to assess the performance of the design proposal, which is detailed in section 3.3. Eventually, section 4 analyses the various influences of key parameters on the resistance, such as strain hardening, section slenderness and shape or local plate buckling. § 4.4 finally presents comparison results with the proposed approach to existing design recommendations.

2 Numerical models – Parametric studies

2.1 General

All non-linear F.E. simulations reported in the present paper have been led by means of non-linear F.E. software FINELg (1999), continuously developed at the University of Liège and Greisch Design Office since 1970. Use of quadrangular 4-nodes plate-shell finite elements with typical features (Corotational Total Lagrangian formulation, Kirchhoff's theory for bending) has been made; mesh sensitivity analyses have been performed and adequate numbers of integration points in-plane and across the thickness have also been adopted.

Both Linear Buckling Analyses (L.B.A., i.e. critical load calculations) and Geometrically and Materially Non-linear with Imperfections Analyses (G.M.N.I.A.) have been performed. L.B.A. calculations resorted to the so-called subspace iteration method coupled with Jacobi eigenvalues extraction technique and Sturm sequences; G.M.N.I.A. analyses were based on state-of-the-art numerical techniques and strategies: pure Newton-Raphson iterative scheme with out-of-balance residuals corrections, associated with the arc-length method and automatic loading strategies up to peak loads and beyond.

As such stainless steel sections are assumed to be fabricated by welding, no particular treatment of the web-flange area was accounted for, contrary to the need to account for the presence of fillets for hot-rolled profiles (Gérard 2019). Accordingly, a little material overlap in these areas occurred, with little influence on the results presented here.

Last, the length of each numerical specimen was set so as to (i) reproduce cross-sectional behaviour as much as possible (i.e. specimens were chosen long enough to shy away from edge effects but short enough to avoid member buckling) and to (ii) comply with recommended geometrical local imperfection patterns – see § 2.4.

2.2 Material response

Stainless steel being an iron-based alloy containing a minimum of 11% chromium, different chemical compositions are usually met in various material grades: austenitic, ferritic, duplex, martensitic, martensitic-austenitic, etc. In order to limit the number of F.E. calculations without disregarding too much of the available stainless steel grades, only grades 1.4003, 1.4301 and 1.4362 were considered in the parametric studies, being deemed the most common and representative.

Each material model was represented by a so-called two-stage model (Gardner 2002) that follows the well-known Ramberg-Osgood expression up to $\sigma_{0.2}$ but adopts a modified equation beyond $\sigma_{0.2}$ and up to the ultimate stress, as follows (Gardner 2004):

$$\left\{ \begin{array}{l} \varepsilon = \frac{\sigma}{E_0} + 0.002 \cdot \left(\frac{\sigma}{\sigma_{0.2}} \right)^n \quad \text{for } \sigma \leq \sigma_{0.2} \\ \varepsilon = \frac{(\sigma - \sigma_{0.2})}{E_{0.2}} + \left(0.008 - \frac{\sigma_{1.0} - \sigma_{0.2}}{E_{0.2}} \right) \cdot \left(\frac{\sigma - \sigma_{0.2}}{\sigma_{1.0} - \sigma_{0.2}} \right)^{n'_{0.2,1.0}} + \varepsilon_{i,0.2} \quad \text{for } \sigma \geq \sigma_{0.2} \end{array} \right. \quad (1)$$

Where $E_{0.2} = \frac{\sigma_{0.2} \cdot E_0}{\sigma_{0.2} + 0.002 \cdot \ln E_0}$

Fig. 2a further illustrates the material responses of the three grades considered in the numerical studies. In practice, the materials laws for the 3 stainless steel grades considered were implemented in the F.E. models through the use of 8 linear segment approximations per curve, as Fig. 2b shows. The slope of each segment was optimised through linear regression analysis,

and Fig. 2a and 2b show an excellent level of accordance. In particular, smaller segments were used in the most rounded parts of the curves.

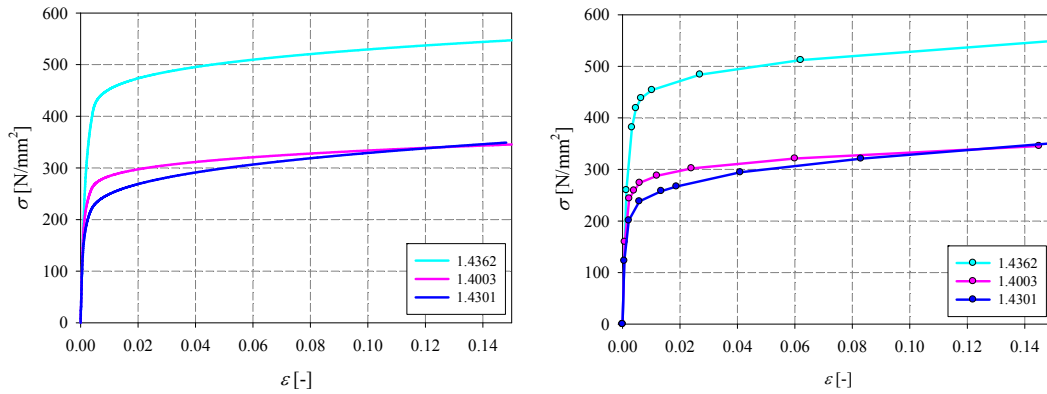


Figure 2: a) Original σ - ε relationship (two-stage R.-O.) – b) 8-segment approximations for F.E. simulations

2.3 Loading and support conditions

Regarding support conditions accounted for in the shell models, two main aspects have been distinguished for the definition of the reference “fork conditions” at the member’s ends. The first one concerns the treatment of in-plane cross-sectional local supports: these have been defined as Fig. 3 shows, and consequently provide (i) local lateral support to possible local buckling owing to concentrated support reactions, as well as (ii) global cross-section fork condition supports, namely fixing lateral and vertical deflections, as well as torsional twist.

The second aspect deals with the possible axial displacements (“ x -oriented”) of the end cross-section nodes. In order to allow for a maximum number of four global degrees-of-freedom of the end cross-section (i.e. axial displacement, rotations θ_y , θ_z and warping, so as to keep the shell modelling similar to typical beam-like assumption such as Bernoulli’s in bending), use of linear kinematic constraints has been made between the flange and web nodes. While a maximum of four nodes may experience a “free” longitudinal displacement, all other nodes’ x -displacements linearly depend on the longitudinal displacements of the “ x -free” nodes to respect a global cross-sectional displaced configuration – see also (Gérard 2019) for more details.

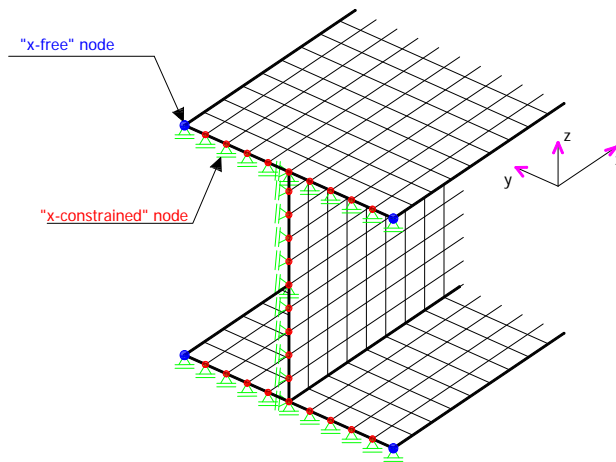


Figure 3: Modelling of end sections: transverse supports and linear constraints (longitudinal)

For symmetry reasons, the four nodes at the flanges tips have been chosen as the “ x -free” ones, and all other nodes are consequently the “ x -constrained” ones. Doing so allows for a sufficiently

correct treatment of the global cross-section behaviour, given the usual levels of displacements and rotations reached within present study. It also avoids the usual technique of superposing additional stiff elements along the flanges and webs of the end-sections that aim at preventing local instabilities but may generate numerical troubles. This modelling technique has been shown to be very effective from a numerical point of view and was validated and adopted in many F.E. studies (Greiner et al., 2009).

2.4 Imperfections

Associated to the fabrication process considered here, a typical welded residual stresses pattern was introduced in the models, in all G.M.N.I.A. calculations (see Fig. 4a). Amplitudes and distribution shapes follow carbon steel recommendations (ECCS 1976), as observed by Bredenkamp et al. (1992); albeit relatively usual, this pattern bears the particularity that self-equilibrium is ensured on a plate-per-plate basis, through adequate values of γ_1 and γ_2 that depend of the section's dimensions.

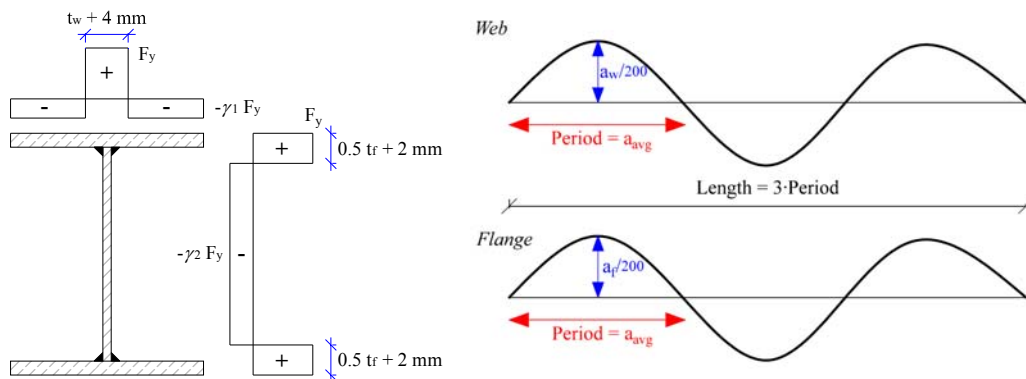


Figure 4: a) Residual stresses pattern considered (welded) – b) Definition of geometrical local imperfections

As for geometrical imperfections, a specific sub-study was carried out to help make a decision on which standard distributions shall be used along the main F.E. parametric studies. These preliminary investigations were indeed motivated by a general lack of knowledge in the field for stainless steel sections (Ashraf 2006) as well as by quite different ways of dealing with the definition of both shape and amplitude of the local geometrical imperfections.

Indeed, for more classical carbon steel sections, various recommendations set the amplitude of the initial local imperfection to be made dependent on the plate dimensions – see for example (EN1993-1-5 2005, Pavlovic 2005, Beg et al. 2010 or Johansson et al. 2007) –, while others relate it to the plate thickness t – more precisely to a function of t , see (Gardner 2010, Dawson 1972, Schafer 1998) for example. While both dependencies make sense and can be justified from a mechanical point of view, relative little correlation with t could be observed for stainless steel sections (Gardner 2004). Besides, the selection of an appropriate shape for the initial geometrical imperfection may also either be based on the 1st eigenmode (or a combination of several modes) or on sine distributions (see Nseir 2015, Gérard 2019b).

Accordingly, the following dedicated preliminary study was carried out, comprising the following parameters:

- 12 different section sizes (6 “beam shapes” IPE sections + 6 “column shapes” HEA sections), including invented sections obtained from regular ones with a 30% reduction of all thicknesses – sections denoted with ‘ and “ in the following. These sections were intended to get results for cases where local buckling and the associated initial imperfections is more influential while keeping other dimensions constant, in particular the h / b ratios;

- 2 load cases, either simple compression N or major-axis bending M_y ;
- 4 different amplitudes of geometrical local imperfections, all based on sinusoidal patterns along both dimensions of the plates by adequate modification of node coordinates: first, two amplitudes as functions of thickness t were considered (as recommended by Ashraf 2006): $0.1 t$ and $0.5 t$. The second set of amplitudes consisted in functions of plates' leading dimension a , with either $a / 100$ or $a / 200$.

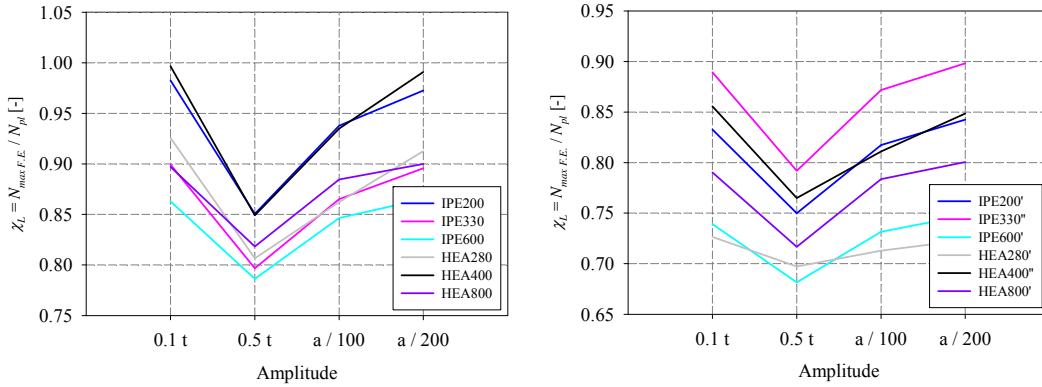


Figure 5: Results of imperfection study – a) Catalogue shapes – b) Invented (more slender) sections

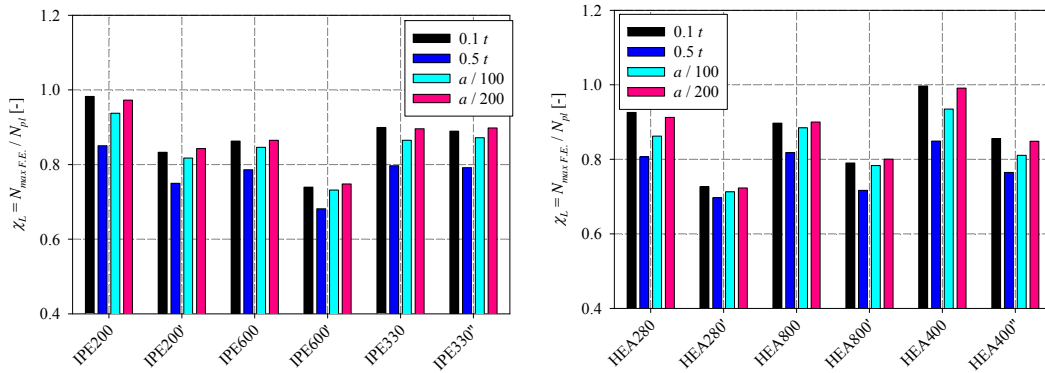


Figure 6: Influence of local imperfection amplitude (sections in compression) – a) Beam shapes – b) Column shapes

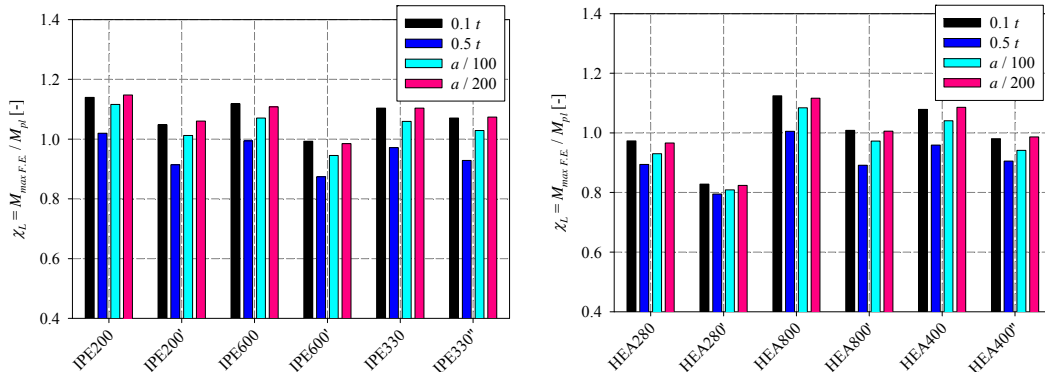


Figure 7: Influence of local imperfection amplitude (sections under major-axis bending) – a) Beam shapes – b) Column shapes

Overall, 96 F.E. simulations were performed. Results are presented in Figs. 5 to 7, for all sections considered – including invented, more slender ones, and for N and M load cases. All

results refer to χ_L which is defined as the ratio between the numerically-obtained peak load and the corresponding plastic capacity, i.e. χ_L stands as the “local buckling factor”. χ_L values below unity therefore indicate a detrimental influence of local buckling, while $\chi_L > 1.0$ denote benefits from material strain hardening.

The obtained results show that the various possibilities considered with respect to the amplitude yield similar and consistent results for all section shapes – including for the invented ones –, for both N and M load cases, at the exception of cases with $0.5 t$ amplitudes which are always the most detrimental, by far. These tendencies were expected, as amplitudes as high as $0.5 t$ may be quite exaggerated compared to measured data (Greiner et al. 2009). Also, it appears clearly from Fig. 5b that the more slender invented sections for which the value of the amplitude is decisive also provide coherent results for all amplitudes tested but $0.5 t$. Therefore, this possible amplitude choice shall be disregarded, and was not kept any further.

Additionally, as will be detailed in the next § 2.5, the present study intends at embracing quite slender cross-sections, so that a dependency on a rather than on t was preferred. Again, since measured initial geometrical imperfections data and even some design codes (EN1993-1-5 2005) encourage preferring $a / 200$, the latter recommendation was followed within the main parametric studies described in the next paragraph.

2.5 Parametric studies

As based on the previously-detailed F.E. models, an extensive numerical parametric study was carried out, encompassing the following main parameters:

- Material laws: the 3 different grades detailed previously were accounted for (grades 1.4301, 1.4003 and 1.4362 with respective equivalent 0.2% proof-stresses of 210 N/mm², 250 N/mm² and 400 N/mm²;
- Section dimensions (welded open sections): a total of 50 different sections was considered:
 - 10 beam-type girders (i.e. with height-to-width ratios $h / b \approx 2$), from the European Section catalogue IPE family: IPE80, IPE140, IPE160, IPE240, IPE270, IPE300, IPE330, IPE450, IPE550 and IPE600;
 - 10 column-type sections ($h / b \approx 1$): HEA140, HEA240, HEA280, HEA400, HEA500, HEA650, HEA700, HEA800, HEA900 and HEA1000;
 - 10 heavy sections geometries (large thicknesses so as to observe the biggest possible influence of material strain hardening): HEM140, HEM240, HEM280, HEM400, HEM500, HEM650, HEM700, HEM800, HEM900 and HEM1000;
 - 10 more slender IPE shapes obtained from the regular series but accounting for a 30% reduction in thickness of both web and flanges (designated as IPES in the following, S referring to more Slender geometries);
 - 10 more slender HEA shapes with similarly reduced thicknesses (denoted as HEAS)
- Two simple load cases, either sections in compression (N) or under major-axis bending (M);
- Both L.B.A. and G.M.N.I.A. computations were contemplated, in order to get (i) the (local) critical load multiplier $R_{cr,L}$ (cf. Figs 1 and 8) as well as the (ii) ultimate load multiplier (carrying capacity).

Some 75 simulation results were also added through more slender section geometries lying in between usual beam and column shapes, i.e. slender sections with ratios h / b intermediate between 1.0 and 2.0 – see § 4.2 for more analysis details. Each G.M.N.I.A. computation

accounted for the imperfection patterns detailed previously, and a total of about 750 non-linear results was collected, and are further analyzed and detailed in Section 4.

3 Analytical resistance predictions

3.1 Current design provisions in major standards

All F.E. results gathered were compared to existing design provisions for stainless steel sections, following the recommendations of the European (EN1993-1-4 2006) and American (AISC 2010) codes, as well as to C.S.M.-based resistance predictions.

Eurocode 3 Part 1.4 design rules for stainless steel remain in large amounts inspired by carbon steel ones: first, like many modern design codes, it relies on the concept of classes to characterize section resistance as a function of the sensitivity to local buckling. Although not appropriate for sections made of materials with no yield plateau (Boissonnade 2017, Chen 2013), classification still is a preliminary step to the determination of the resistance of stainless steel sections, and leads to either plastic, elastic or effective resistance of the section.

The plastic resistance of stainless steel sections in Eurocode 3 – denoted EC3 in the following – keeps being based on assumed constant stress blocks associated to the proof stress $\sigma_{0.2}$, and does not account for any further strain hardening effects. Accordingly, EC3 predictions are expected to be safe-sided for the most compact section shapes, e.g. for HEM sections. As per slender sections, EC3 makes use of the Effective Width Method (E.W.M.), based on Von Karman’s approach that consists in neglecting the contribution to resistance of fibres in areas supposedly most affected by local buckling.

Partly similar to the EC3 approach, the U.S. design requirements (denoted AISC hereafter) for stainless steel are also based on the concept of classes, and requires the E.W.M. for compression cases but relies on “simplified” procedures in bending where the tedious calculations associated to the E.W.M. are avoided. Instead, sets of approximate equations depending on the pair classes of flanges and web are provided. Here again, strain hardening effects are not specifically addressed.

3.2 Continuous Strength Method

In contrast, the Continuous Strength Method (C.S.M., Gardner 2008) proposes a radically different, strain-based design approach. The basic principles and application steps of the C.S.M. consist in (i) relying on an experimentally-calibrated base curve relating the plate slenderness of the leading cross-section plate to the strain ratio $\epsilon_{peak} / \epsilon_{yield}$, then (ii) distribute stresses and strains across the section from ϵ_{peak} and (iii) integrate the material model through the section assuming linear strain distributions (Bernoulli assumption) so as to provide a C.S.M. resistance prediction.

Accordingly, the classification step is no longer necessary and the C.S.M. nicely provides continuous strength predictions from plastic to slender capacities. Also, use of an experimentally-based $\epsilon_{peak} / \epsilon_{yield}$ ratio allows to better account for the influence of the material behaviour on the section’s overall response, i.e. potential strain-hardening benefits are duly considered.

Resistance predictions from both the C.S.M., EC3, AISC and the proposed O.I.C.-based approach described in the next paragraph are compared to the F.E. reference results in § 4.4.

3.3 O.I.C. approach – Design proposal

As summarized previously, the O.I.C. approach provides direct resistance predictions from so-called χ - λ “buckling” curves. In the particular case of cross-section resistance, reference shall

be made to *local* buckling, and factors $R_{cr,L}$, λ_L and χ_L are of concern – see Fig. 8. In the same way as the C.S.M., continuous resistance predictions are ensured through a continuous buckling curve, and section classification is no more necessary. Although reference shall classically be made to the 0.2% proof stress $\sigma_{0.2}$, the rounded material response, including strain hardening effects, can efficiently be accounted for through adequate definitions of the buckling curves, possibly allowing for $\chi_L \geq 1.0$ values, i.e. section capacity may exceed plastic resistance. As another key feature, the case of slender sections is also easily and straightforwardly accounted for without resorting to the E.W.M., and direct resistance predictions are provided.

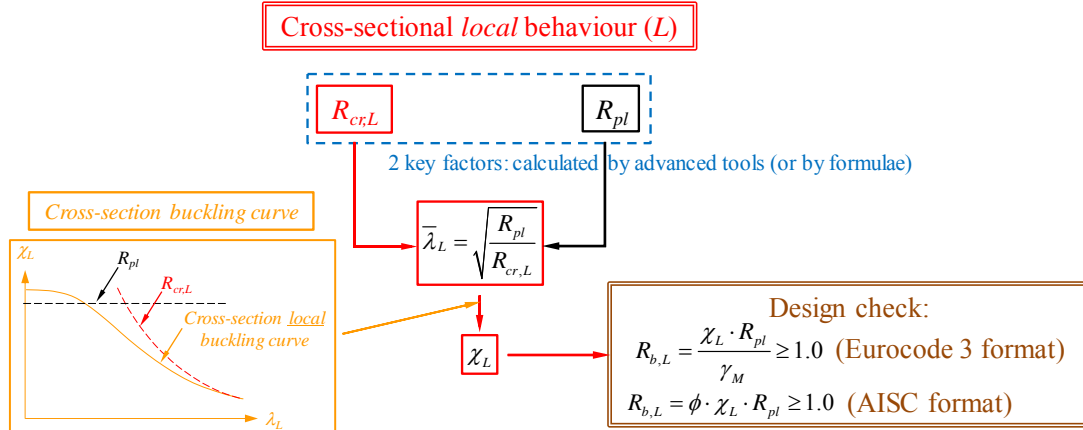


Figure 8: O.I.C. design chart for cross-sectional *local* resistance

Table 1: design equations for O.I.C.-based approach

	Compression N	Major-axis bending M
General definitions	$\lambda_L = \sqrt{\frac{R_{pl}}{R_{cr,L}}} = \sqrt{\frac{N_{pl}}{N_{cr,L}}}$ $\lambda_0 = 0.45$	$\lambda_L = \sqrt{\frac{R_{pl}}{R_{cr,L}}} = \sqrt{\frac{M_{pl}}{M_{cr,L}}}$ $\lambda_0 = 0.50$
Cases for which $\lambda_L \leq \lambda_0$		
Stainless steel grade	Compression N	Major-axis bending M
1.4301	$\chi_L = 0.13 \cdot \ln(137 \cdot e^{-8.5 \cdot \lambda_L}) + 0.85$	$\chi_L = 0.15 \cdot \ln(0.45 \cdot \lambda_L^{-2}) + 0.91$
1.4003	$\chi_L = 0.1 \cdot \ln(65 \cdot e^{-6.8 \cdot \lambda_L}) + 0.89$	$\chi_L = 0.11 \cdot \ln(0.45 \cdot \lambda_L^{-2}) + 0.94$
1.4362	$\chi_L = 0.13 \cdot \ln(49.6 \cdot e^{-6.2 \cdot \lambda_L}) + 0.86$	$\chi_L = 0.13 \cdot \ln(0.45 \cdot \lambda_L^{-2}) + 0.93$
Cases for which $\lambda_L \geq \lambda_0$		
General definitions	$\gamma = \frac{\sigma_{cr,w}}{\sigma_{cr,f}} = \frac{\sigma_{cr,w}}{\sigma_{cr,f}} \cdot \left(\frac{b_f \cdot t_w}{h_w \cdot t_f} \right)^2$ $\phi_L = 0.5 \cdot (1 + \alpha_L \cdot (\lambda_L - \lambda_0) + \lambda_L^\delta)$ $\chi_L = \frac{1}{\phi_L + \sqrt{\phi_L^2 - \lambda_L^\delta}}$	
	Compression N	Major-axis bending M
	$\alpha = 0.4 \cdot \gamma + 0.06$	$\alpha = 0.22 \cdot \gamma + 0.0091$
	$\delta = 0.45 \cdot \gamma + 0.023$	$\delta = 0.15$

Accurate definitions of – *local* – buckling curves is therefore essential. In the present context, two sets of definitions, depending on local cross-section slenderness λ_L , have been proposed:

- For quite compact sections characterized by $\lambda_L \leq \lambda_0$ where λ_0 is a reference cross-sectional slenderness (cf. Table 1), $\lambda_L \geq 1.0$ values are proposed through equations that have been calibrated on the basis of a strain-based approach similar to the C.S.M. (see details on Figs. 10a to 10d). For an improved accuracy, the proposed expressions have been made dependent on the stainless steel grade and on the load case;
- For sections with $\lambda_L \geq \lambda_0$, the influence of local buckling becomes more detrimental and a classical, Ayrton-Perry buckling curve format is proposed (see Table 1), which is characterised by (i) the use of factor δ that accounts for post-buckling resistance reserves (Nseir 2015) and by (ii) a dependency on parameter γ which takes the balance of the susceptibility to buckling of the respective plate constituent elements.

The merits of the proposed design approach as well as the influence of many factors such as the steel grade, cross-section shape or plate buckling are detailed in the next Section; accuracy and performance of the proposal is also compared to existing approaches. Finally, it shall also be noted that in the present study, all R -factors associated to the O.I.C. approach have been calculated by means of accurate tools (purposely-developed software), for an improved precision – such tools are currently being finalised and shall be made available soon; alternatively, as specified in Fig. 8, approximate formulae may be used, e.g. cross-section plastic interaction equations for R_{pl} or critical stresses for $R_{cr,L}$, see (Boissonnade 2017).

4 Analysis of results – Accuracy of proposal

4.1 Influence of strain-hardening

As of prime importance, the ability of the design proposal to take advantage of stainless steel material response and strain hardening effects is firstly investigated here. Figs 9a and 9b plots the obtained results in typical relative resistance-slenderness χ_L - λ_L axes, where, in addition, so-called “Resistance” $\chi_L = 1.0$ and “Stability” curves are reported: the “Resistance” limit is to be associated with R_{pl} and characterizes the attainment of the full plastic capacity (i.e. no influence of buckling) while the “Stability” limit represents the 1st order linear buckling maximum capacity characterized by R_{cr} (i.e. no yielding, allowable stress is infinite).

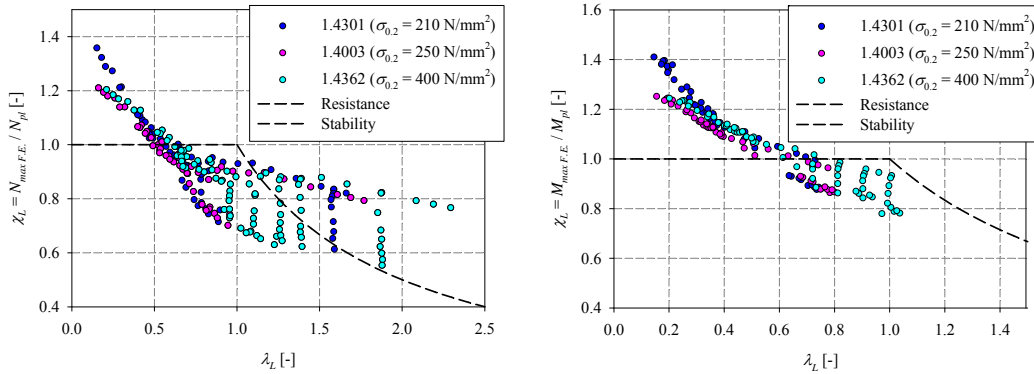


Figure 9: Influence of steel grade on resistance a) Sections in compression – b) Sections under major-axis bending M_y

As the figures show, the general distribution of results is quite scattered, especially for compression load cases and for high values of the section slenderness ($\lambda_L > 1.0$) where significant changes in resistance are noted for a given λ_L . As expected, important benefits from strain hardening are also observed, obviously in regions of low slenderness; results show up to

40% higher carrying capacity than the plastic resistance in some cases. Also, regardless of the steel grade, an important amount of results lies above the $\chi_L = 1.0$ limit ($\lambda_L < 0.45$ cases for compression and $\lambda_L < 0.5$ sections under major-axis bending). This further confirms that stainless steel sections may be utilized beyond their plastic capacity as based on $\sigma_{0.2}$ and that the associated increase in resistance provides non negligible benefits, given the relative expensive costs of stainless steel.

For the latter $\lambda_L \leq \lambda_0$ cases, the O.I.C. equations proposed in Table 1 have been calibrated with these numerical results, as Figs. 10a to 10d show. A two-step procedure was followed, where $\varepsilon_{peak} / \varepsilon_y$ is firstly made a function of λ_L , and then χ_L a function of $\varepsilon_{peak} / \varepsilon_y$. As can be seen, a difference was made between steel grades for compression cases (Fig. 10a), but not for bending cases (Fig. 10c).

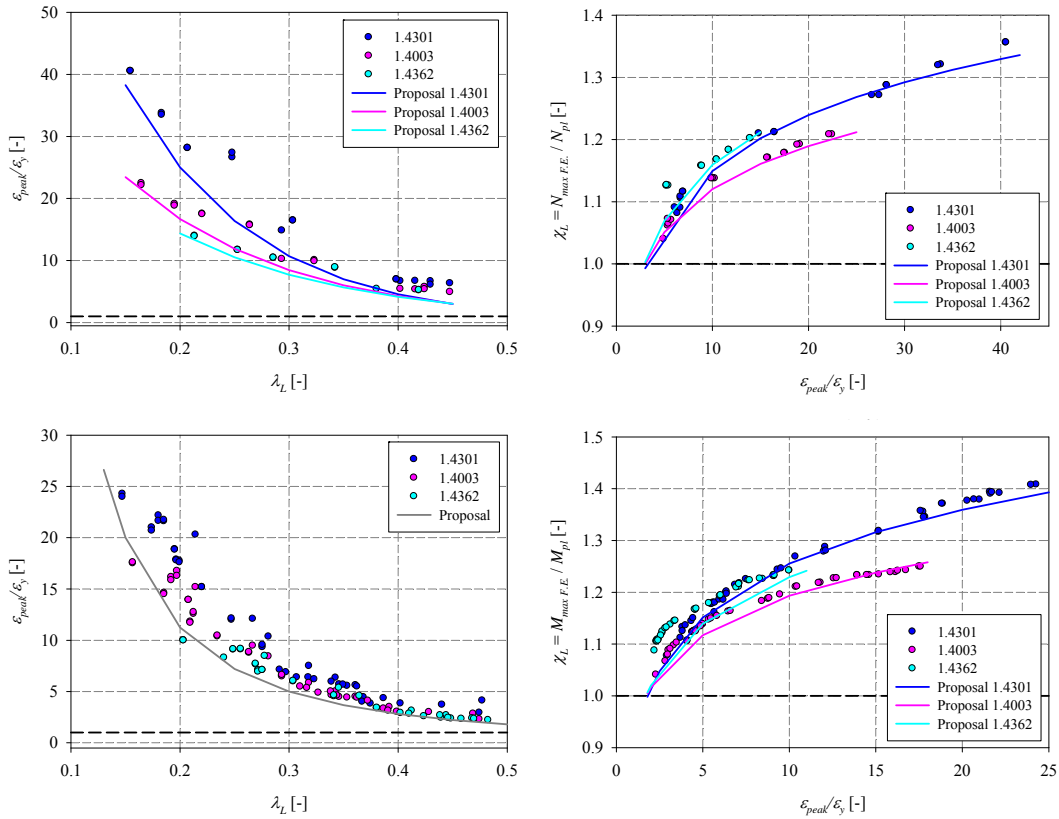


Figure 10: strain-based approach in O.I.C. method for low slenderness (resistance higher than plastic)

a) and b): Design approach for compression – c) and d): Design approach for major-axis bending

The more scattered results of Fig 9 in regions of moderate to (very) slender sections arise from other influences, as the next paragraphs show.

4.2 Influence of section slenderness and shape

Figs. 11a and 11b propose a plotting of the same results, where however a distinction is made between sections' shapes. Especially for the compression load case, this is seen to be a key parameter explaining the disparity of the results: in general, IPE sections (beams) provide higher resistances than their HEA (columns) counterparts, for an identical λ_L . Albeit IPES and HEAS inverted sections nicely complement the observed trends and allow to deal with more slender sections, a non-negligible resistance gap between these families of section shapes is clearly visible, both for compression and bending cases. In this respect, additional sections have

again been invented so as to provide intermediate data – namely through varying the height-to-width ratio h/b . Besides, nearly all section shapes are seen to be positively affected by strain hardening reserves, HEM sections obviously being the ones taking the most advantage of these.

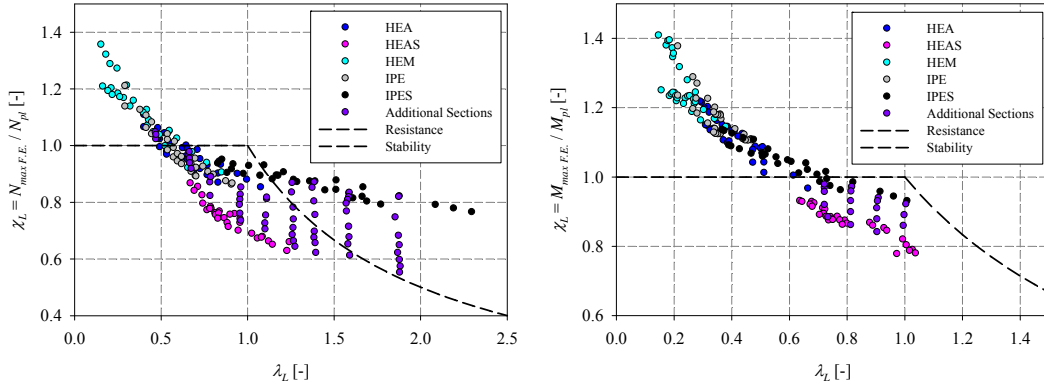


Figure 11: Influence of section shape on resistance a) Sections in compression – b) Sections under major-axis bending M_y

Consequently, it appears justified that O.I.C. design equations relating χ_L to λ_L shall be made dependent on the section’s aspect ratio or on any other parameter somehow related. Fig. 12a shows how the simple aspect ratio parameter h/b allows for this, although a bit roughlyly.

For the particular case of carbon steel sections, Gérard (2019c) suggested resorting to parameter $(b \cdot t_f^2) / (h \cdot t_w^2)$ which, beyond the h/b ratio, further accounts for the influence of web and flanges relative thicknesses. Fig. 12b illustrates how relying on this parameter may efficiently help providing transitional resistances between beam and column shapes. However, in the present study, another parameter γ was preferred, as mentioned in § 3.3 and further analyzed in the next paragraph.

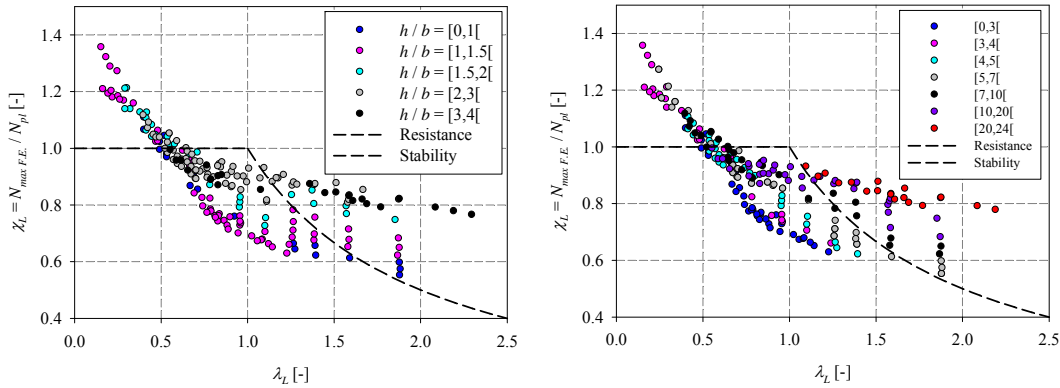


Figure 12: Adequacy of various parameters to provide transitional resistances from beam to column shapes (compression cases considered) – a) Parameter h/b – b) $(b \cdot t_f^2) / (h \cdot t_w^2)$

4.3 Effect of individual plate buckling on section response

Figs. 13a and 13b further allow to understand how the sensitivity to local buckling of individual plates (i.e. web and flanges) rule the resistance shift from beam to column shapes. Indeed, these figures display a very good ability of parameter γ to sort the results (see definition of γ in Table 1); γ being defined as the ratio of respective web and flange critical stresses, the beam-shape or column-shape response of sections at moderate to high slenderness is found governed by individual plate buckling, i.e. a single plate element may govern the entire section’s response in cases of typical IPE or HEA dimensions: a low value of γ indicates that local buckling in the

web rules the section's response (e.g. IPE sections in compression) while a high γ relate to flange-driven cases (e.g. HEA in compression or bending).

The figures also allow to preliminarily assess the performance of the proposed design approach for cases where local buckling becomes detrimental – situations where $\chi_L < 1.0$. Results sorted by ranges of γ (e.g. $\gamma = [0-0.01[$) can be compared to their corresponding interval's lower bound curve, to observe a general very good accordance.

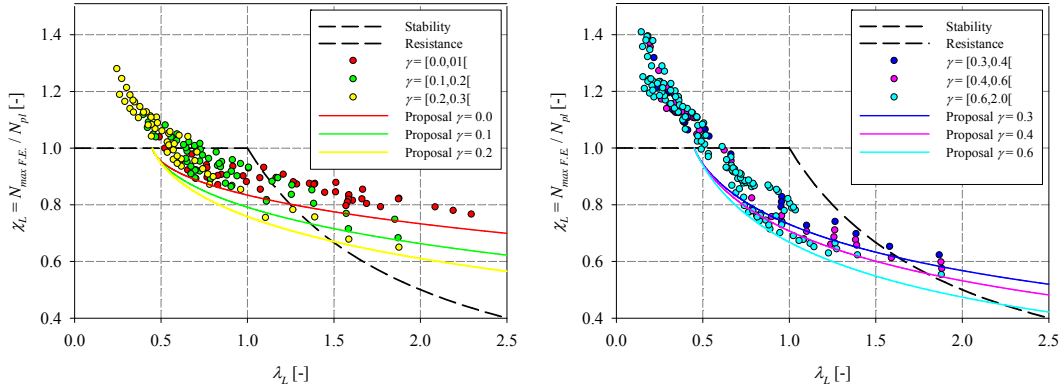
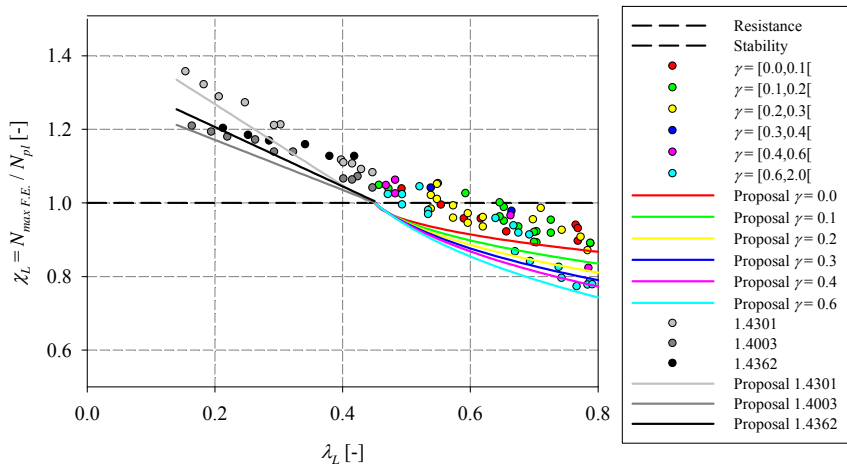


Figure 13: Correlation between resistance and section shape through proposed parameter γ

More advanced attempts towards relying on more accurate (and complex) expressions for $\sigma_{cr,w}$ and $\sigma_{cr,f}$ allowing for plate interactions were also experienced through the use of software EBPlate (2017) and web-flange interaction diagrams (Trahair et al. 2007). The intention was to investigate whether the assumption of isolated plates within the section – leading to constant k_σ factors – should beneficially be substituted by a more realistic one acknowledging for plate element interaction at the cross-section level. Results indicated that little benefits in accuracy were brought by such more complex approaches, therefore the simpler design approach suggested in § 3.3 where γ is defined with classical plate theory k_σ factor values was kept.

Figs. 14a and 14b further focus on the performance of the proposed O.I.C. equations for $\lambda_L \leq \lambda_0$ cases, for both compression and major-axis bending cases, respectively. As can be observed, the proposed approach leads to safe and accurate resistance predictions, for all stainless steel grades considered and for both sections in compression and for sections under major-axis bending moment.



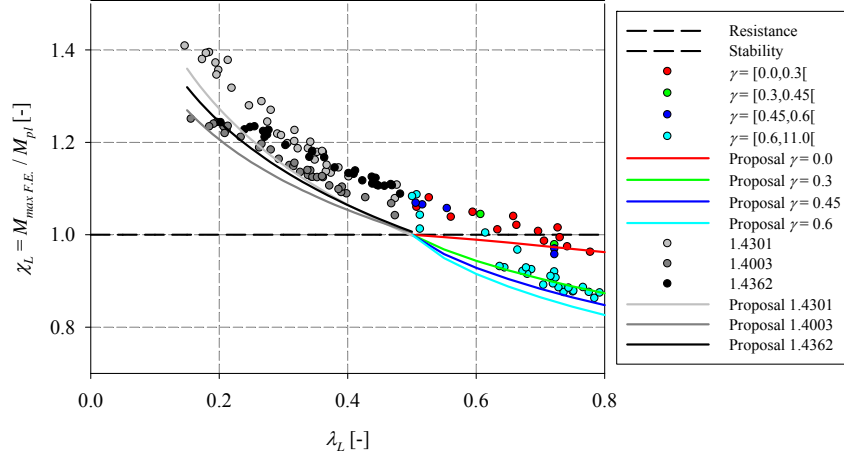


Figure 14: Performance of O.I.C. proposal for low to intermediate cross-section slenderness – a) Sections in compression – b) Sections under major-axis bending moment

4.4 Comparison with existing design approaches and proposal

This last section is devoted to assessing and comparing the performances of the various design approaches described herein with respect to the database of reference F.E. results. Figs. 15a and 15b first analyse the ability of EC3 design rules to provide accurate and safe resistance estimates, through plotting the evolution of the $\chi_{L.F.E.} / \chi_{L.EC3}$ ratio as a function of λ_L ; values of this ratio above unity indicate safe EC3 resistance predictions, while values lower than 1.0 refer to unsafe ones.

As a matter of fact, EC3 provisions are seen poorly appropriate, leading to quite overly-conservative estimates (especially for bending) as well as to quite unsafe ones lying beyond what could possibly be compensated by usual values of safety factor γ_M . In particular, EC3 rules are seen unsuitable at low slenderness where strain hardening is more significant, as was expected. For sections under major-axis bending moment, the results remain very scattered and unduly over-conservative, in large extents owing to the inappropriate discrete behavioral classes concept. The very conservative results at $\lambda_L \approx 0.6$ can indeed be shown to arise from EC3's sudden drop of resistance between M_{pl} and M_{el} that obviously bear no physical meaning and is not visible in the numerical results.

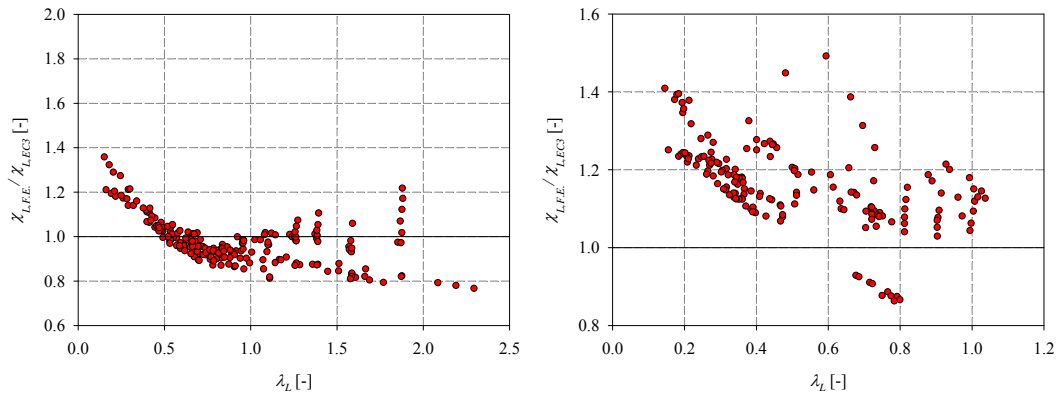


Figure 15: EC3 predictions vs. F.E. reference results – a) Sections in compression – b) Sections under major-axis bending

Fig. 16a and 16b propose a statistical summary of these results, where cumulative frequencies are reported as a function of ranges of the $\chi_{L.F.E.} / \chi_{L.EC3}$ ratio. For sections in compression,

Fig. 16a further evidences a non-negligible amount of results lower than 0.9 for which a $\gamma_M = 1.1$ value may not be sufficient to regain safety. As for Fig. 16b, it mostly emphasizes the scattered results and the high amount of very conservative results with $\chi_{L,F.E.} / \chi_{L,EC3}$ ratios larger than 1.2.

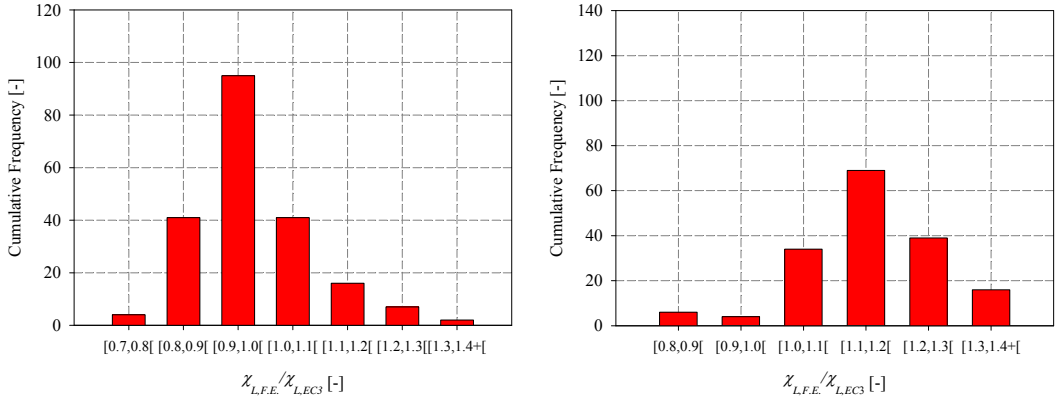


Figure 16: Statistical distribution of $\chi_{L,F.E.} / \chi_{L,EC3}$ ratios – a) Sections in compression – b) Sections under major-axis bending

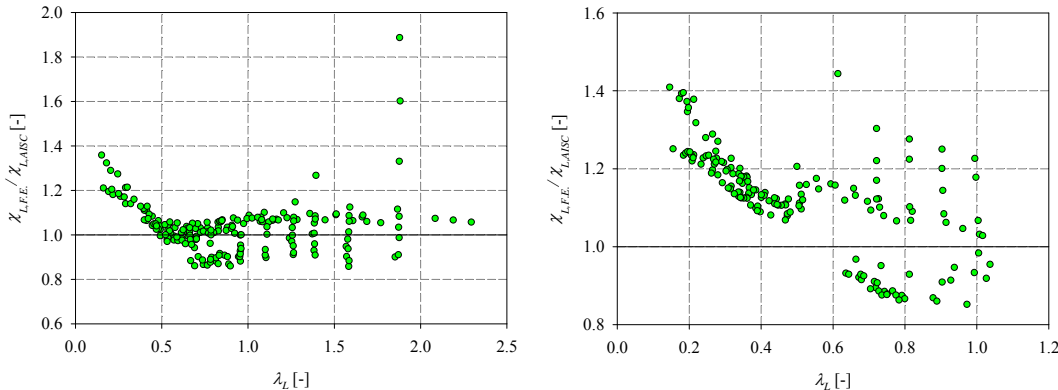


Figure 17: AISC predictions vs. F.E. reference results – a) Sections in compression – b) Sections under major-axis bending

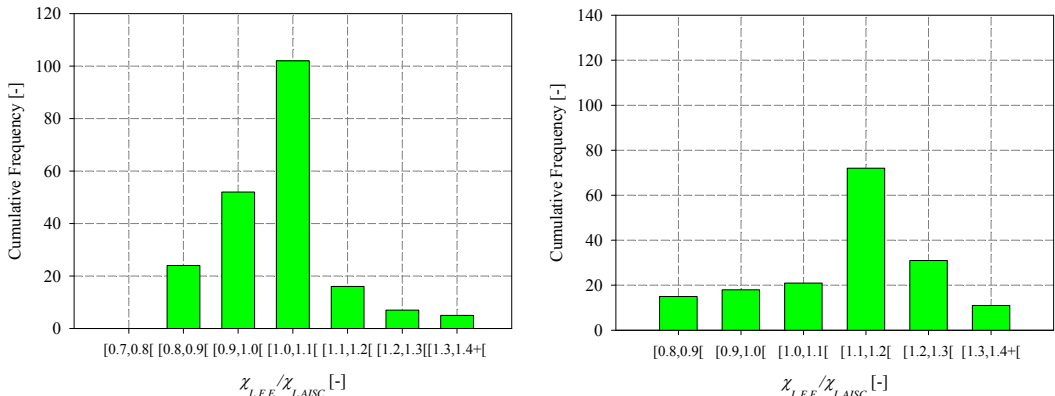


Figure 18: Statistical distribution of $\chi_{L,F.E.} / \chi_{L,AISC}$ ratios – a) Sections in compression – b) Sections under major-axis bending

Similarly, the AISC design provisions exhibit rather poor performances, in nearly the same extents – inability to account for strain hardening at low section slenderness, important unsafe predictions for sections in compression and scattered, over-conservative resistance estimates

for sections under major-axis bending, see Figs. 17a and 17b. Fig. 18a and 18b statistical plots however denote slightly more consistent results in compression but inversely more dispersed tendencies for bending.

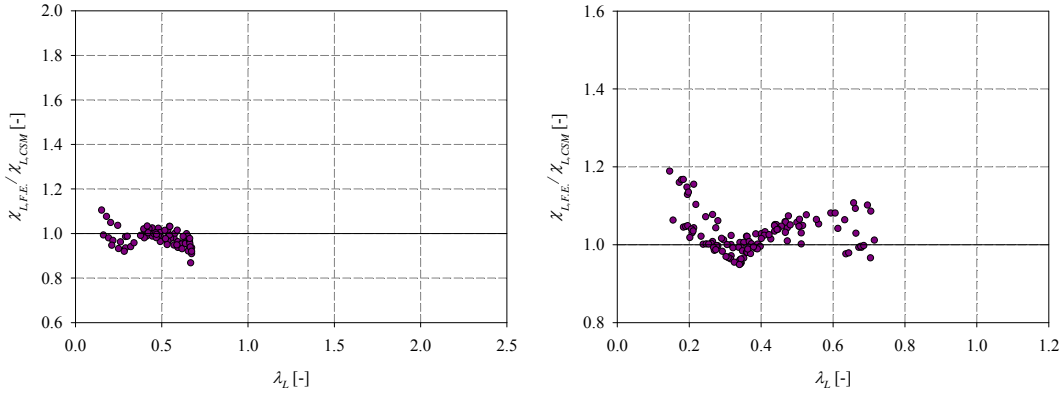


Figure 19: CSM predictions vs. F.E. reference results – a) Sections in compression – b) Sections under major-axis bending

In contrast, the C.S.M. predictions, as reported in Figs 19a and 19b, provide much more accurate and consistent resistance predictions. However, the C.S.M. base curve and the associated predictions remaining limited to λ_L values of max. 0.68, only a limited number results can be reported.

Figs. 20a and 20b finally plot the results of the comparison between the proposed O.I.C. predictions and the F.E. results. For compression load cases, the proposed approach is seen safe, accurate and consistent, along the whole slenderness range, for all section shapes – including the invented, more slender ones – and whatever the steel grade. In particular, the effects of strain hardening at low slenderness and post-buckling reserves for high slenderness are seen to be accurately accounted for. Similar conclusions can be drawn for sections under major-axis bending, at the exception of several data points with high γ values for which the design proposal provides overly safe estimates – this last point is presently under scrutiny.

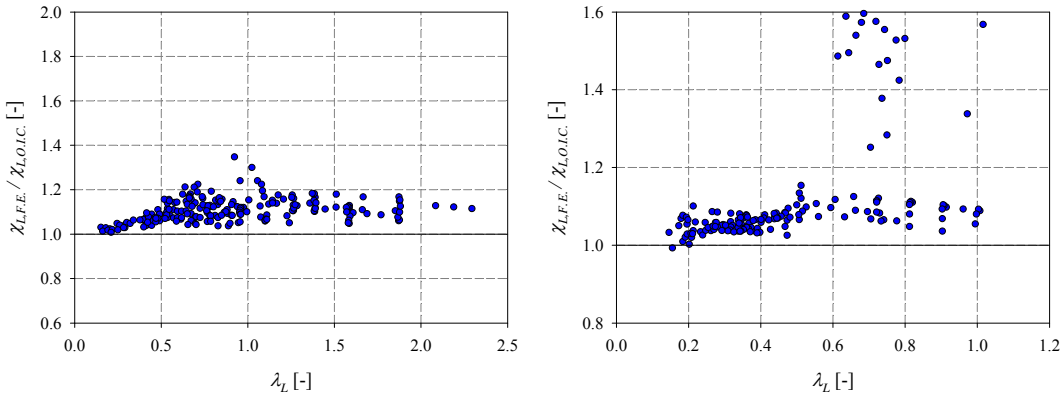


Figure 20: O.I.C. proposal predictions vs. F.E. reference results – a) Sections in compression – b) Sections under major-axis bending

Figs. 21a and 21b statistical plots further confirm the excellent performances of the proposed O.I.C. design approach, since the vast majority of resistance predictions are seen consistent and grouped, lying within 20% of the reference F.E. ones, and always on the safe side.

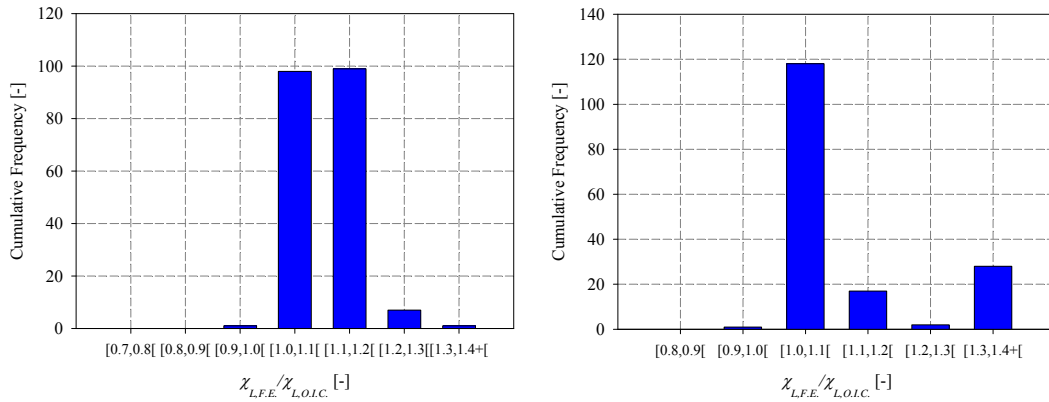


Figure 21: Statistical distribution of χ_{LFE} / χ_{LOIC} ratios – a) Sections in compression – b) Sections under major-axis bending

5 Conclusions

This paper showed how a new direct design approach, following the O.I.C. principles and design steps, can efficiently characterize the resistance of stainless steel sections in compression or under major-axis bending. Confronted to some 750 carefully-conducted shell F.E. simulations, the proposed design equations showed safe, accurate and consistent. In particular, they were evidenced to adequately account for the specific rounded material response and allow for higher resistance levels stemming from pronounced strain hardening effects when relevant. Also, the various influences of section slenderness, of section shape and dimensions or of steel grade were analysed in more details, and the proposed design approach revealed fully appropriate with respect to each parameter. Comparisons with European and American stainless steel specifications also displayed the improved performance of the proposal, both regarding accuracy, consistency and safety aspects.

6 References

- Afshan, S., Gardner, L. (2013). “The continuous strength method for structural stainless steel design”, *Thin-Walled Structures*, vol. 68, pp. 42-49.
- AISC (2010). “Specification for structural steel buildings”, American Institute of Steel Construction, Chicago, IL.
- ANSI/ASIS 360-10 & AISC Design Guide 27 (2013), “Structural Stainless Steel”.
- AS 4100 (1998). “Australian Standard AS 4100 Steel Structures”.
- Ashraf, M. (2006). “Structural Stainless Steel Design: Resistance Based on Deformation Capacity”, PhD thesis, Imperial College London.
- Ashraf, M., Gardner, L., Nethercot, D. (2006b). “Compression strength of stainless steel cross-sections”, *Journal of Constructional Steel Research*, vol. 62, pp. 105-115.
- Beg, D., Kuhlmann, U., Davaine, L., Braun, B. (2010). “Design of Plated Structures. Eurocode 3: Design of Steel Structures, Part 1-5 – Design of Plated Structures”, *ECCS Eurocode Design Manuals*, Eds Ernst & Sohn, ISBN 978-92-9147-100-3.
- Boissonnade, N., Nseir, J., Hayeck, M., Saloumi, E. (2014). “Predicting steel member carrying capacity by means of the Overall Interaction Concept”, *Proceedings of the 7th European Conference on Steel Structures, Eurosteel 2014*, Naples, Italy.
- Boissonnade, N., Hayeck, M., Saloumi, E., Nseir, J. (2017). “An Overall Interaction Concept for an alternative approach to steel member design”, *Journal of Constructional Steel Research*, vol. 135, pp. 199-212.
- Bredenkamp, P. J., van den Berg, G. J., van der Merwe, P. (1992). “Residual stresses and the strength of stainless steel I-section columns”, *Proceedings of the Structural Stability Research Council, Annual Technical Session*, Pittsburg, USA, pp. 69-86.

- Chen, Y., Cheng, X., Nethercot, D. (2013). “An overview study on cross-section classification of steel H-sections”, *Journal of Constructional Steel Research*, vol. 80, pp. 386-393.
- Dawson, R. G., Walker, A. C. (1972). “Post-buckling of geometrically imperfect plates”, *Journal of the Structural Division, ASCE*, vol. 98, No. 1, pp. 75–94.
- ECCS – Committee 8 – Stability. (1976). “Manual on Stability of Steel Structures”, European Convention for Constructional Steelwork.
- EN1993-1-4 (2006). “Eurocode3: Design of steel structures – Part 1-4: General rules –Supplementary rules for stainless steels”, Brussels, European Committee for Standardization (C.E.N.).
- EN 1993-1-5 (2005). “Eurocode 3: Design of Steel Structures, Part 1-5: Plated structural elements”.
- Gardner, L. (2002). “A new approach to structural stainless steel design”, Ph.D. Thesis, Structures Section, Department of Civil and Environmental Engineering, Imperial College London, U.K.
- Gardner, L., Nethercot, D. (2004). “Numerical Modeling of Stainless Steel Structural Components – A Consistent Approach”, *Journal of Structural Engineering*, vol. 130, No. 10, pp. 1586-1601.
- Gardner, L., Talja, A., Baddoo, N. (2006). “Structural design of high-strength austenitic stainless steel”, *Thin-Walled Structures*, vol. 44, pp. 517-528.
- Gardner L., Theofanous, M. (2008). “Discrete and continuous treatment of local buckling in stainless steel elements”, *Journal of Constructional Steel Research*, vol. 64, pp. 1207-12016.
- Gardner, L. (2008b). “The Continuous Strength Method”, *Proceedings of the ICE – Structures and Buildings*, vol. 161, pp. 127-133.
- Gardner, L., Saari, N., Wang, F. (2010). “Comparative experimental study of hot-rolled and cold-formed rectangular hollow sections”, *Thin-Walled Structures*, vol. 48, No. 7, pp. 495–507.
- Gérard, L., Li, L., Kettler, M., Boissonnade, N. (2019). “Recommendations on the definition of material imperfections for the stability and resistance of I and H sections”, submitted to the *Journal of Constructional Steel Research*.
- Gérard, L., Li, L., Kettler, M., Boissonnade, N. (2019b). “Recommendations on the definition of geometrical imperfections for the stability and resistance of I and H sections”, submitted to the *Journal of Constructional Steel Research*.
- Gérard, L., Li, L., Kettler, M., Boissonnade, N. (2019c). “Design of hot-rolled and welded steel open-sections under simple load cases by means of the Overall Interaction Concept”, submitted to the *Journal of Constructional Steel Research*.
- Greiner, R., Kettler, M., Lechner, A., Freytag, B., Linder, J., Jaspert, J.-P., Boissonnade, N., Bortolotti, E., Weynand, K., Ziller, C., Oerder, R. (2009). “SEMI-COMP: Plastic member capacity of semi-compact steel sections – A more economic design”, Research Fund for Coal and Steel, European Commission, ISBN 978-92-79-11113-6, 139 pages.
- Greisch Design Office, University of Liège. (1999). “FINELg, Non Linear Finite Element Analysis Software”.
- Hayeck, M. (2016). “Development of a New Design Method for Steel Hollow Section Members Resistance”, PhD thesis, University of Liège, Belgium.
- Hayeck, M., Nseir, J., Saloumi, E., Boissonnade, N. (2018). “Experimental characterization of steel tubular beam-columns resistance by means of the Overall Interaction Concept”, *Thin-walled Structures*, vol. 128, pp. 92-107.
- Johansson, B., Maquoi, R., Sedlacek, G., Müller, C., Beg, D. (2007). “Commentary and worked examples to EN 1993-1-5, Plated Structural Elements”, 1st Edition, ECCS-JRC Report No. EUR 22898 EN.
- Li, L., Gérard, L., Hayeck, M., Boissonnade, N. (2017). “Stability of slender section HSS columns”, *Proceedings of the Annual Stability Conference, Structural Stability Research Council, San Antonio, Texas*.
- Nseir, J., Saloumi, E., Hayeck, M., Boissonnade, N. (2015). “A new design method for hollow steel sections: the Overall Interaction Concept”, *Proceedings of the 15th International Symposium on Tubular Structures, ISTS15, Rio de Janeiro, Brazil*.
- Nseir, J. (2015b). “Development of a New Design Method for the Cross-section Capacity of Steel Hollow Sections”, PhD thesis, University of Liège, Belgium.

- Pavlovic, L. (2005) "Shear resistance of longitudinally stiffened webs of plated girders", PhD thesis, University of Ljubljana; Slovenia.
- Real, E., Mirambell, E. (2005). "Flexural behaviour of stainless steel beams", *Engineering Structures*, vol. 27, pp. 1465-1475.
- Schafer, B., Peköz, T. (1998). "Computational modelling of cold-formed steel: Characterizing geometric imperfections and residual imperfections", *Journal of Constructional Steel Research*, vol. 47, pp. 193–210.
- Software EBPlate, v2.01, Centre Technique Industriel de la Construction Métallique, France.
- Theofanous, M., Gardner, L. (2010). "Experimental and numerical studies of lean duplex stainless steel beams", *Journal of Constructional Steel Research*, vol. 66, pp. 816-825.
- Trahair, N., Bradford, M., Nethercot, D., Gardner, L. (2007). "The Behaviour and Design of Steel Structures to Eurocode 3", 4th edition, Taylor & Francis.
- Young, B., Liu, Y. (2003). "Experimental investigation of cold-formed stainless steel columns", *Journal of Structural Engineering*, vol. 129, pp. 169-176.
- Young, B., Lui, W.M. (2005). "Behavior of cold-formed high strength stainless steel sections", *Journal of Structural Engineering*, vol. 131, pp. 1738-1745.